SUPPLEMENTARY MATERIAL

Supplementary material and methods:

- Computational details: Molecular Dynamics (MD) simulation was performed for the system CA32F1 to investigate the effect of the introduction of the large side chain of Arg162. After appropriate preparation of the system as explained in the main manuscript an orthorhombic water box with a minimum distance of 10 Å was introduced. The system was then neutralized and 150 mM NaCl added. Equilibration using the default protocol was performed followed by 20 ns NPT simulation at 300 K and 1 atm using DESMOND software.58 with the OPLS- 2005 force field51. The temperature was regulated with the Nosé-Hoover chain thermostat59, with a relaxation time of 1.0 ps, while the pressure was controlled by the Martyna−Tobias−Klein barostat60 with isotropic coupling and a relaxation time of 2.0 ps. The RESPA integrator61 was employed with bonded, near, and far time steps of 2.0, 2.0, and 6.0 fs, respectively. A 9 Å cutoff is used for non-bonded interactions together with the smooth particle mesh Ewald method.62

To minimize the effects of manually introduced mutation V162AR (given the significant change in side chain size) in the model system of CA32F1 we have performed a 20 ns MD simulation. The simulation, shown to stabilize after about 5 ns (**Fig. S6**) contains an initial orientation of the R162 side chain, placed with Maestro software, that changes along the simulation. Initially, the CZ atom of the guanidino group is about 8 Å away from the carboxylic group of both D205 and E164, as can be seen in **Fig. S7**. Throughout the simulation it is seen that the loop in which both R162 and E164 are located is very flexible allowing for a diversity of possible arrangements. Two main conformations are observed: one where the R162 is interaction with E164 (between 4 to 11 ns and 13 until 15 ns) and R162 and D205 are between 6 and 11 Å away, and a second where the three amino acids are interacting from 15ns until the end of the simulation. We have selected the last configuration from the MD simulation to use in PELE calculations and have observed that also in PELE simulations this loop is very flexible and all conformations observed in MD are reproduced.

Supplementary Tables

Table S1. Primers used for mutagenesis of the six residues of the substrate binding pocket of 3A4 laccase

Primer	5'-3' sequence
mut162-164-F	GCTGCCAAAGTCGGCCCGGCGNNKCCGNNKGCCGATGCTACTCTTATCAAC
mut162-164-R	GTTGATAAGAGTAGCATCGGCMNNCGGMNNCGCCGGGCCGACTTTGGCAGC
mut263-264-F	CTACTGGATCCGTGCCCTTCCCNNKNNKGGGACCAGGAACTTCGACG
mut263-264-R	CGTCGAAGTTCCTGGTCCCMNNMNNGGGAAGGGCACGGATCCAGTAG
mut390-392-F	CTCCCCGCCACCTCCGCCGCCNNKGGCNNKCCGCACCCCTTCCACTTG
mut390-392-R	CAAGTGGAAGGGGTGCGGMNNGCCMNNGGCGGCGGAGGTGGCGGGGAG
RMLN	CCTCTATACTTTAACGTCAAGG
RMLC	GGGAGGGCGTGAATGTAAGC

Supplementary Schemes

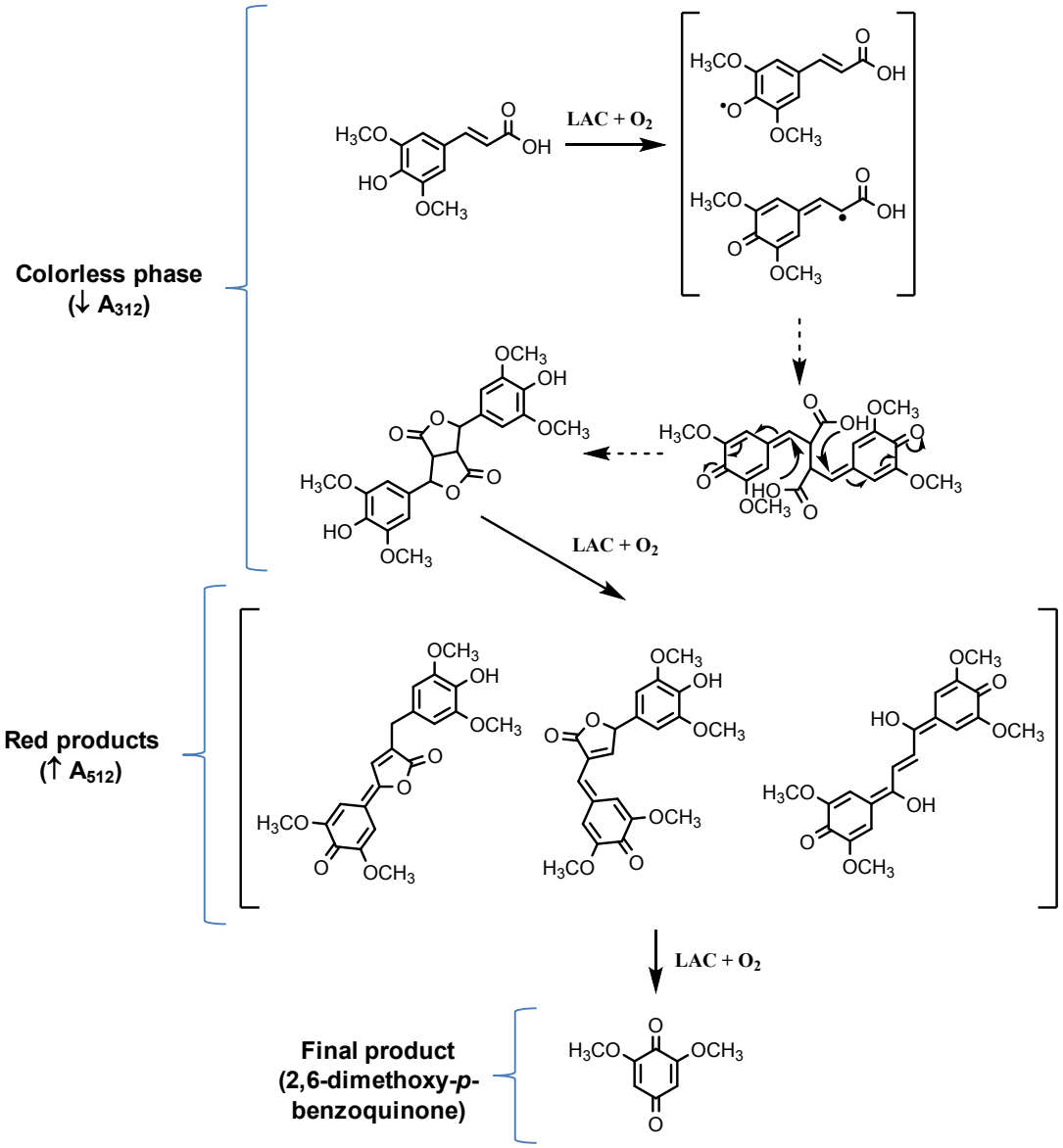

Scheme S1. Reaction pathway for SA oxidation with the main oxidation intermediates as proposed by Lacki and Duvnjak (1998). Solid arrows indicate reaction steps catalyzed by laccase. Dashed arrows indicate non-enzymatic steps.

Supplementary Figures

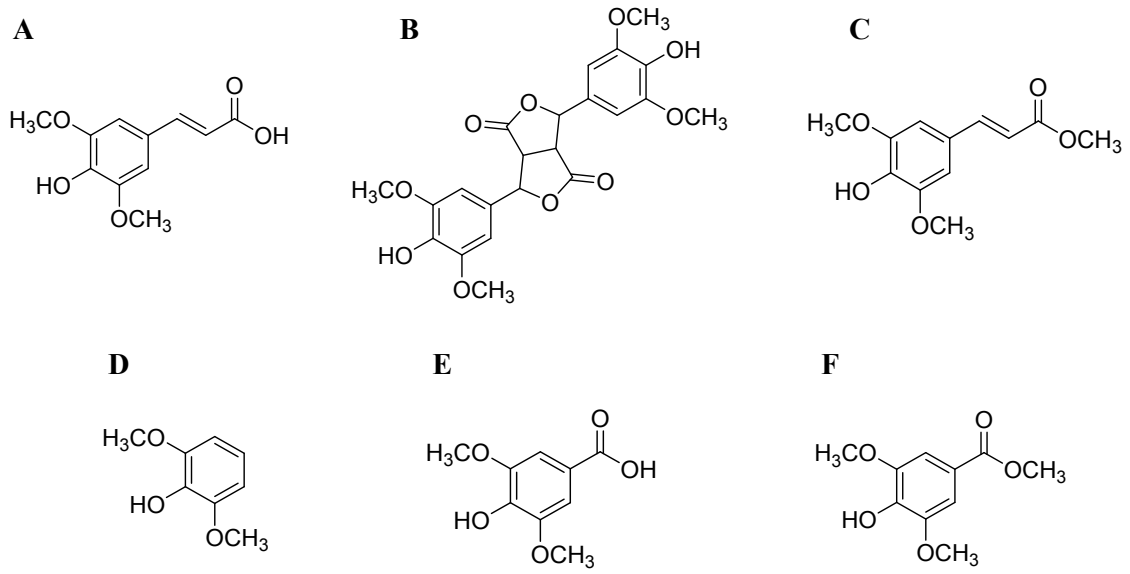

Figure S1. Chemical structures of SA (A), DAD (B), MS (C), DMP (D), SyA (E) and MSy (F).

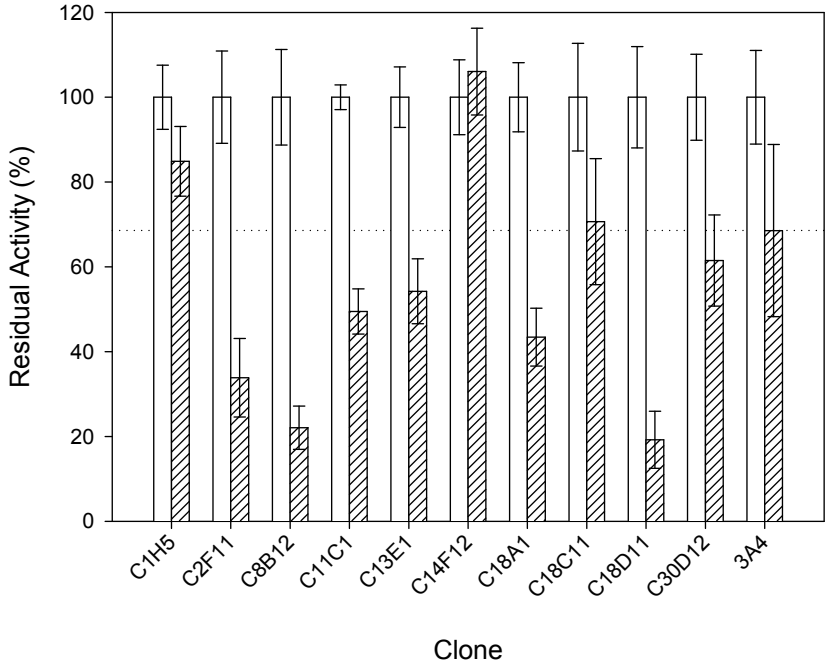

Figure S2. Thermostability screening assay for selected clones from library C. Initial activity and residual activity after 10 min incubation at 71 °C are shown in white and striped bars, respectively. Mean values were obtained from five replicates, error bars represent standard deviations.

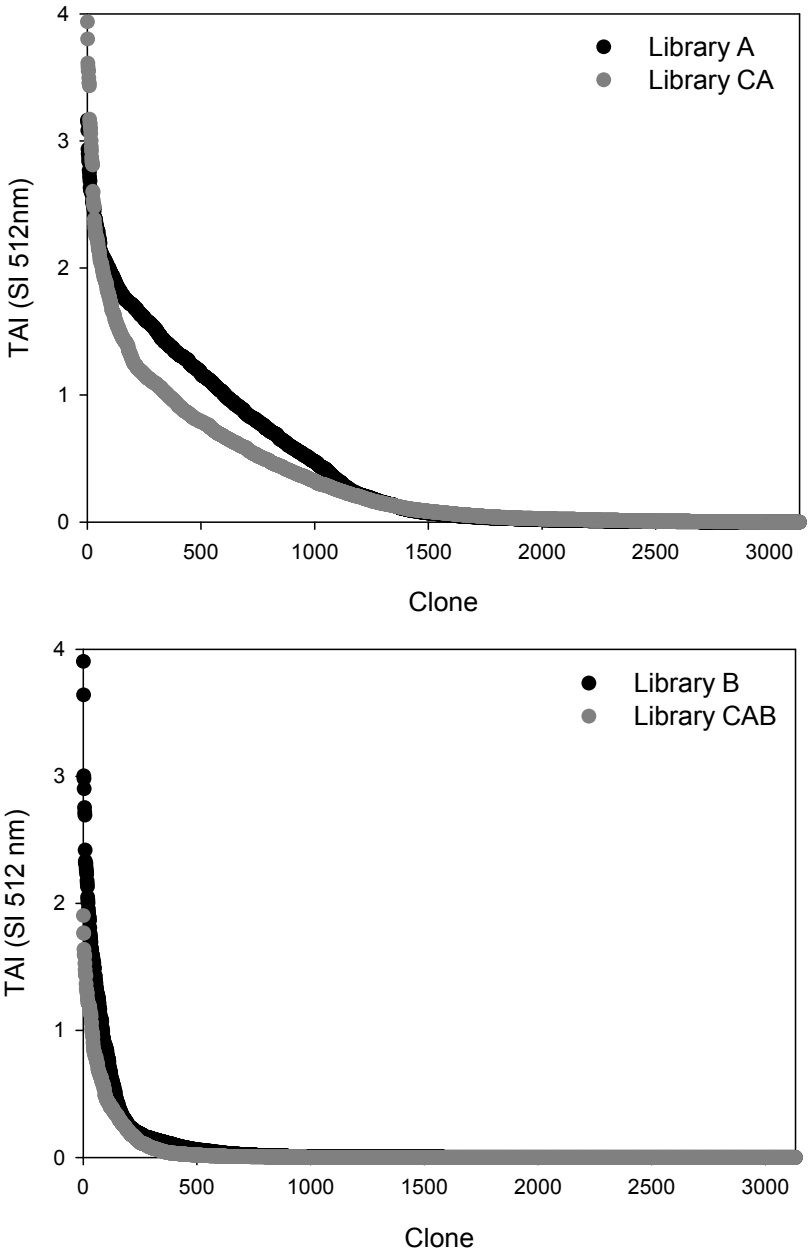

Figure S3. Activity landscapes for mutant libraries A vs CA (A) and B vs CAB (B).

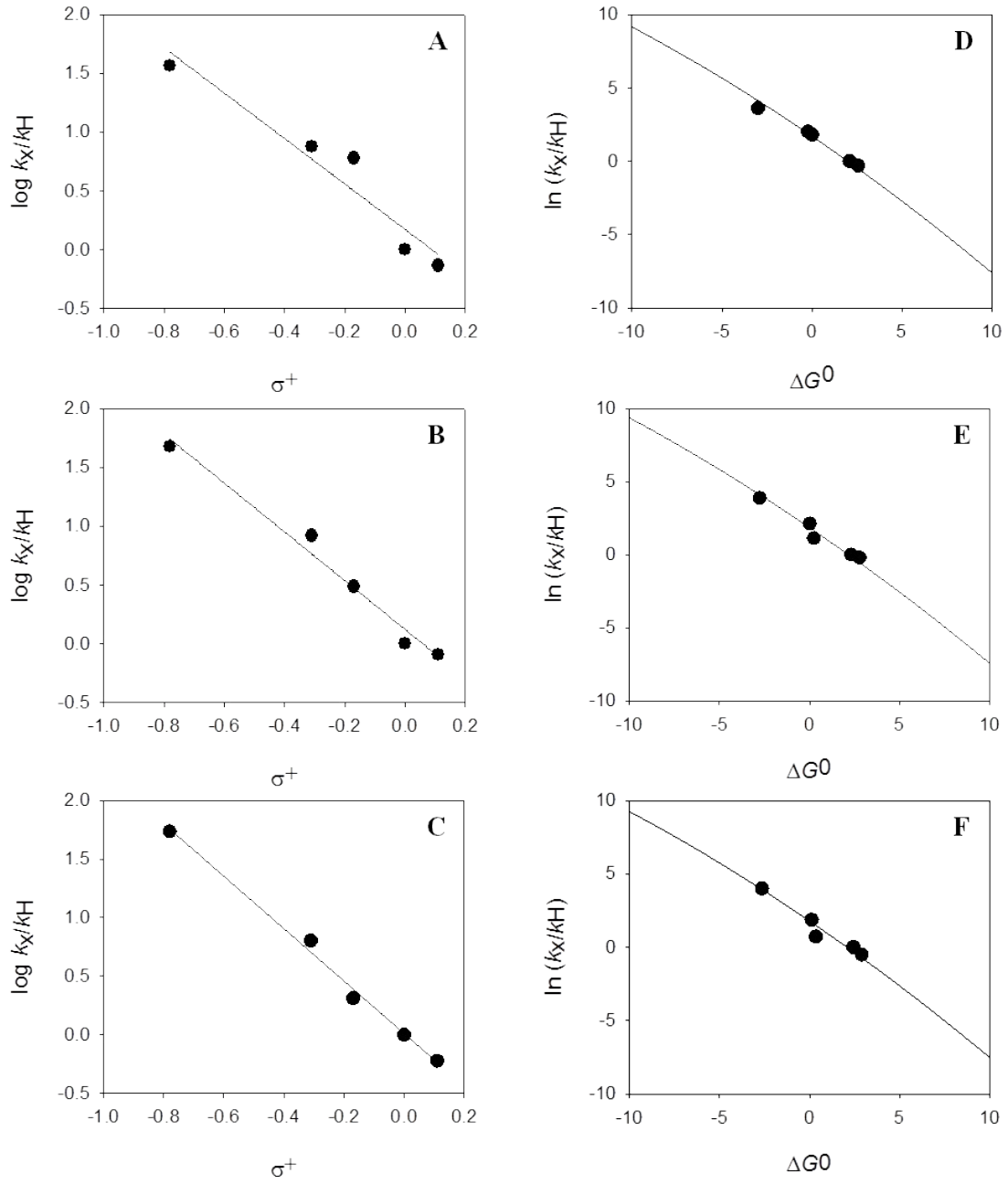

Figure S4. Hammett (A-C) and Marcus (D-F) plots obtained from competition reactions with different p-substituted phenols for laccase variants 3A4 (A, D), C14F12 (B, E) and CA32F1 (C, F).

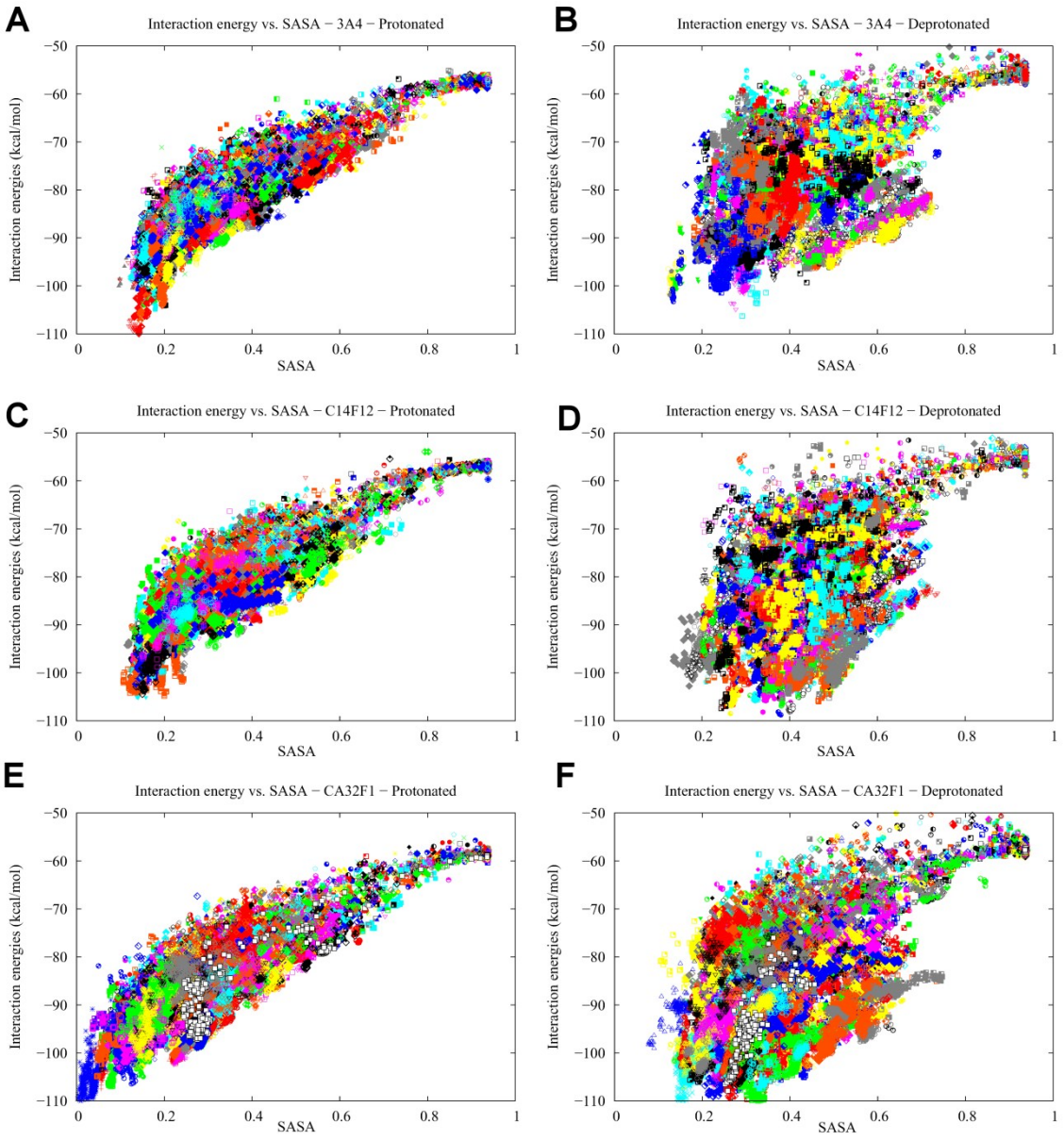

Figure S5. PELE results for the 3A4 (A,B), C14F12 (C,D) and CA32F1 (E,F) variants conformational search of SAH (A,C,E) and SA^- (B,D,F).

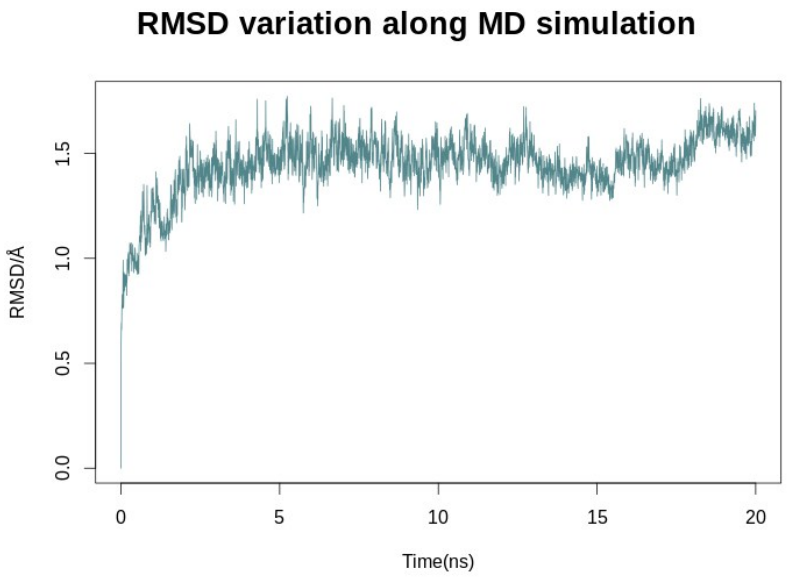

Figure S6. RMSD vs. time for MD simulation of CA32F1

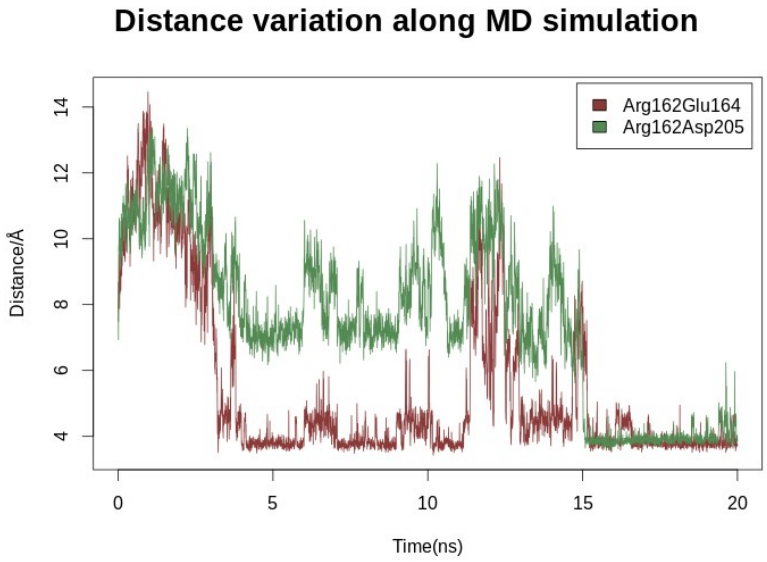

Figure S7. Plot showing how the distance between R162-E164 and R162-E205 vary along the MD simulation of CA32F1.

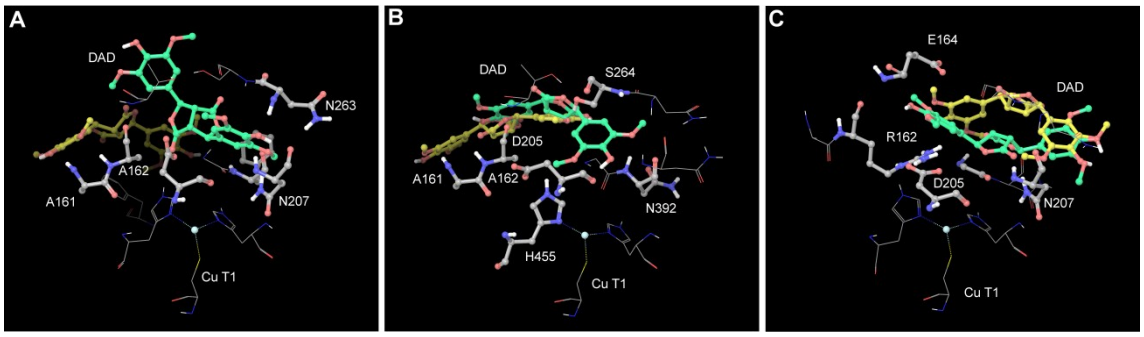

Figure S8. Representative protein-substrate complexes for A) 3A4, B) C14F12 and C) CA32F1 variant with DAD. Each plot represents the best (green) and worse (yellow) position for electron transfer computed with QM/MM.

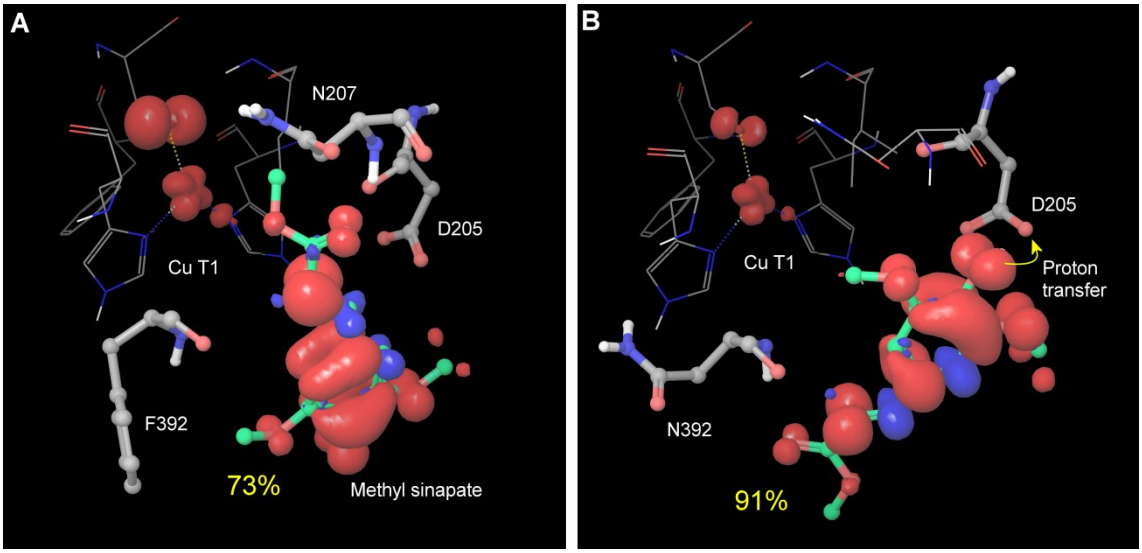

Figure S9. Representative protein-substrate complexes for A) 3A4 and B) C14F12 and MS. Spin density isosurfaces shown in red and blue.